Strojniški vestnik - Journal of Mechanical Engineering 54(2008)12, 866-873
UDC 681.527.34
Paper received: 21.01.2008
Paper accepted: 25.09.2008

Effects of the Variation of Torque Motor Parameters on Servovalve Performance

Dušan Gordić*- Milun Babić - Nebojša Jovičić - Dobrica Milovanović
University of Kragujevac, Faculty of Mechanical Engineering in Kragujevac, Serbia

An electrohydraulic servovalve is an essential item of fluid power servomechanism where fast response, high power output and working fidelity are necessary. Based on detailed and experimentally verified mathematical model of two-stage spool position mechanical feedback electrohydraulic servovalves sensitivity analysis has been performed. The effects of variation of few torque motor electromagnetic parameters (air-gap length (thickness) at null, residual magnetic flux density (magnetic inductivity) of permanent magnet and number of turns of each coil) on dynamic performance of B.31.210.12.1000.U2V PPT servovalve have been studied. Obtained results are in accordance with servovalve engineering design practice.

Keywords: electrohidraulics, servovalves, torque motors, sensitivity analysis

0 INTRODUCTION

Two-stage spool position feedback electrohydraulic servovalves with the torque motor as an electromechanical converter and a flapper-nozzle valve as the first stage of hydraulic amplification are the most utilised servovalves in electrohydraulic control systems for the last forty years. In spite of their relatively long period of application, all phenomena associated with their operation are not completely quantitatively and qualitatively explained. This is due to facts that a relatively complex mathematical apparatus, coming from fundamental laws of electromagnetism, fluid mechanics and general mechanics, is needed for describing their operation. Beside, these mathematical expressions include many parameters that are very difficult to precisely quantify.

In this paper authors study the influence of torque motor electromagnetic parameters on servovalve behaviour. Many authors gave contributions to the explanation of electromagnetic nature of servovalve torque motors. Still Merritt [1] explained in detail the effects of some non-linearities on the servovalve behaviour including torque motor non-linearities (magnetic hysteresis and saturation). In the paper [2], Arafa and Rizk made a special review on torque caused by electromagnetic forces. A non-linear mathematical model based on physical quantities was developed in [3]. This model includes non-linear relations for the torque motor dynamics. From the experimental data and FEA analysis performed in [4], Fussell et al. state that magnetic flux leakage must be considered in the lumped model for torque predictions. In [5] and [6], Urata analysed the torque motor dynamics in detail and influence of unequal air-gap length thickness in null in servo valve torque motors.

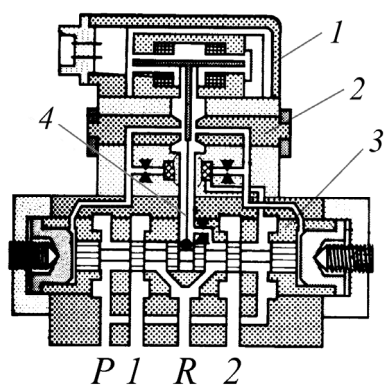

Fig. 1. *Two-stage spool position feedback electrohydraulic servovalve (mechanical feedback) 1 – torque motor, 2 – first stage, 3 – second stage, 4 – feedback spring*

1 THEORETICAL MODEL

Detailed theoretical model should be used in order to investigate the influence of torque motor electro-magnetic parameters on servovalve behaviour. It should include all physical phenomena and torque motor parameters that are

*Corr. Author's Address: University of Kragujevac, Faculty of Mechanical Engineering, Sestre Janjic 6, 34000 Kragujevac, Serbia, gordic@kg.ac.yu

expected to be of influence on behaviour of analysed servovalves.

1.1 Torque Motor

When current is made to flow through torque motor coils, armature ends become polarised. A torque is thus produced on the armature which starts to move. It is common in practice, as it was proved in [7], to use the linear expression to calculate this torque:

$$T_e = K_i i + K_m \theta \,, \tag{1}$$

where values for K_i and K_m are obtained experimentally.

Taking into account expressions for electromagnetic forces in torque motor air gaps, where expressions for magnetic fluxes in air gaps (obtained using the first and the second Kirchhoffs' laws for magnetic circuits) are implemented torque produced on armature can be calculated using (in the case of parallel coil connection):

$$T_e = \frac{r \cdot \mu_0 \cdot A_p}{x_{p0}^2}\left(M_m + N\frac{r\cdot\theta}{x_{p0}} i\right) \cdot \frac{\left[M_m \frac{r\cdot\theta}{x_{p0}} + N(1+k_r)i\right]}{\left[1-\left(\frac{r\cdot\theta}{x_{p0}}\right)^2 + k_r\right]^2} \,, \tag{2}$$

where permanent magnet magnetomotive force is:

$$M_m = \frac{l_m B_{rm}}{\mu_m}\frac{1}{k_m} \,. \tag{3}$$

Linearising Eq. 2 about the null position ($i = 0$ and $\theta = 0$) one can write:

$$K_i = \frac{Nr\mu_0 A_p M_m}{x_{p0}^2\left(1+k_r\right)} \,, \tag{4}$$

$$K_m = \frac{r^2 \mu_0 A_p M_m^2}{x_{p0}^3\left(1+k_r\right)^2} \,. \tag{5}$$

Magnetic reluctance constant k_r considers influences of permanent magnet reluctance, the non-uniformity of a magnetic field through the permanent magnet volume, reduction of the magnetic field in the permanent magnet due to influences of end poles and the leakage flux in air gaps, as it was described in [5]. Following expressions should be used for its calculation:

$$k_r = \frac{R_{mm}}{R_{mp0}}\frac{1}{k_l} \,, \tag{6}$$

where

$$R_{mm} = \frac{l_m}{A_m \mu_m}\frac{1}{k_m} \,, \tag{7}$$

$$R_{mp0} = \frac{x_{p0}}{\mu_0 A_p} \,. \tag{8}$$

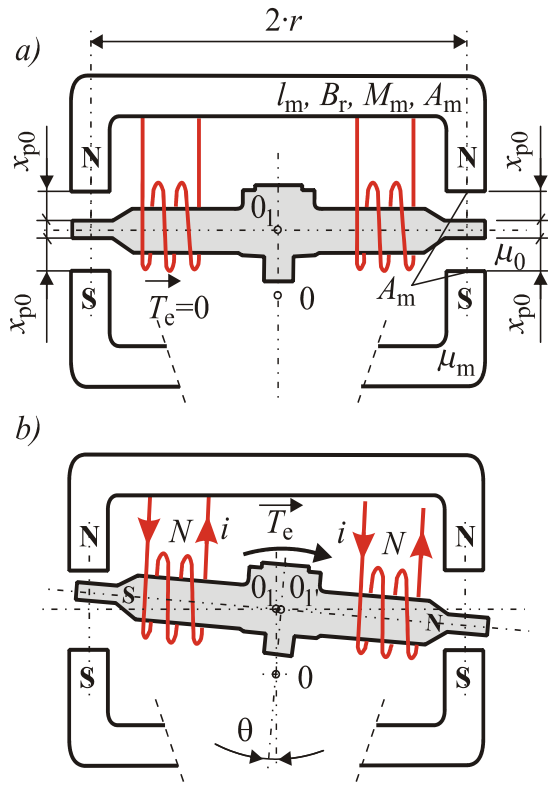

Fig. 2. *Calculation of torque caused by electromagnetic forces in the torque motor: a) neutral, b) current runs through coils*

1.2 Other Parts of the Servovalve

Only final equations of the model are presented in this paper for the reference. Presented equations are related to two-stage electrohydraulic servovalves with mechanical feedback. Detailed explanation of formulae can be found in [8] AND [9].

As long as the flapper does not hit a nozzle, armature dynamics can be described with:

$$T_e = J_a\ddot{\theta} + k_v\dot{\theta} + T_t + F_h l_a + T_f\,, \tag{9}$$

where:

$$l_a = l_{fl} - \frac{l_t}{2}\,. \tag{10}$$

The torque caused by flexure tube deformation can be written as:

$$T_t = \frac{B_t}{l_t}\theta\,. \tag{11}$$

Flow force on the flapper is given by:

$$F_h = (p_l - p_r)\frac{d_n^2\pi}{4} + 8\pi\cdot \left[K_{nl}^2(x_0 - x)^2(p_l - p_d) - K_{nr}^2(x_0 + x)^2(p_r - p_d)\right] \tag{12}$$

where flapper tip displacement is:

$$x = \theta l_a - F_h\left(\frac{l_{fl}^3}{3B_{fl}} + \frac{l_t^3}{12B_t}\right). \tag{13}$$

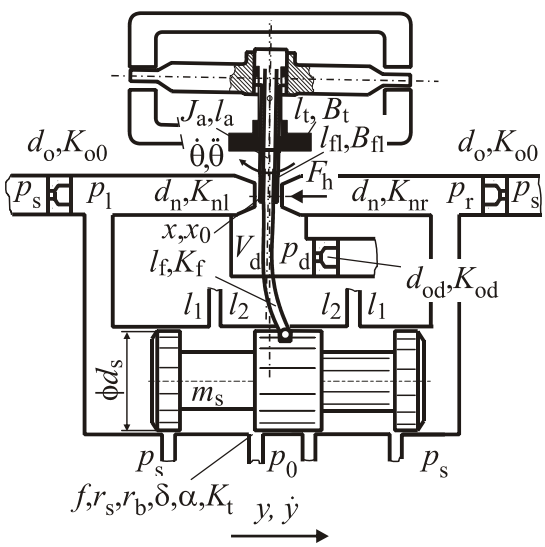

Fig. 3. *Schematic of the servovalve with the parameters of its other parts*

The torque caused by feedback spring deformation can be calculated with:

$$T_f = F_f l_f\,, \tag{14}$$

where the appropriate force is:

$$F_f = \begin{cases} 0 & |y + y_{ff}| < z \\ K_f\left[y + y_{ff} - z\,\mathrm{sgn}(y + y_{ff})\right] & |y + y_{ff}| \geq z \end{cases}. \tag{15}$$

where:

$$y_{ff} = x + l_f\varphi\,, \tag{16}$$

$$\varphi = \theta - \frac{F_h l_{fl}^2}{2B_{fl}}\,. \tag{17}$$

Pressures in flapper-nozzle valve can be obtained using:

$$p_l = \frac{a^2 p_s + b^2 p_d}{a^2 + b^2} + \frac{d^2(b^2 - a^2)}{(a^2 + b^2)^2} - \frac{2abd}{(a^2 + b^2)^2}\sqrt{(a^2 + b^2)(p_s - p_d) - d^2} \tag{18}$$

$$p_r = \frac{a^2 p_s + c^2 p_d}{a^2 + c^2} + \frac{d^2(c^2 - a^2)}{(a^2 + c^2)^2} + \frac{2acd}{(a^2 + c^2)^2}\sqrt{(a^2 + c^2)(p_s - p_d) - d^2} \tag{19}$$

$$[(x_0 - x)\sqrt{p_l - p_d} + (x_0 + x)\sqrt{p_r - p_d}]K_{n0}d_n\cdot \cdot\pi\sqrt{\frac{2}{\rho}} = K_{od}\frac{d_{od}^2\pi}{4}\sqrt{\frac{2}{\rho}}\sqrt{p_d - p_0} + \frac{V_d}{\beta}\dot{p}_d \tag{20}$$

where:

$$a = K_{o0}\frac{d_o^2\pi}{4}\sqrt{\frac{2}{\rho}}\,, \tag{21}$$

$$b = K_{n0}d_n\pi(x_0 - x)\sqrt{\frac{2}{\rho}}\,, \tag{22}$$

$$c = K_{n0}d_n\pi(x_0 + x)\sqrt{\frac{2}{\rho}}\,, \tag{23}$$

$$d = \frac{d_s^2\pi}{4}\dot{y}\,. \tag{24}$$

Algorithm for the calculation of flow coefficients can be found in [8].

The differential equation of spool motion can be written as:

$$\Delta p\frac{d_s^2\pi}{4} = m_s\ddot{y} + k_n\dot{y} + F_c + F_a + F_f\,, \tag{25}$$

where:

$$\Delta p = p_l - p_r\,. \tag{26}$$

Dry friction force can be presented as:

$$F_c = \begin{cases} F_{cn}\,\mathrm{sgn}(\dot{y}), & \dot{y} \neq 0, \\ Z, & |Z| < F_{c0}, \\ F_{c0}\,\mathrm{sgn}(Z), & |Z| \geq F_{c0}, \end{cases} \quad \dot{y} = 0, \tag{27}$$

where:

$$Z = \Delta p \frac{d_s^2 \pi}{4} - F_a - F_f . \quad (28)$$

In the case of the null lap condition for all four symmetrical and matched spool orifices of no-load servovalve, the following expression can be used for the axial component of the flow force:

$$F_a = 2\frac{K_t^2}{K_c} f\, y_i \cos\alpha (p_s + p_0) + \\ + (l_2 - l_1) K_t \sqrt{2\rho (p_s - p_0)} f\, \dot{y} \quad (29)$$

where the real value of spool valve opening is:

$$y_i = \sqrt{(\delta + r_s + r_b)^2 + (|y| + r_s + r_b)^2} - (r_s + r_b) . \quad (30)$$

Numerical data from Dong and Ueno are used for the calculation of jet angle, contraction coefficient and flow coefficient [8].

The volumetric flow through the servovalve can be mathematically formulated as:

$$Q_{SV} = (K_t f y_i \sqrt{\frac{2}{\rho}} \sqrt{\frac{p_s - p_0}{2}} - Q_l)\,\mathrm{sgn}(y) . \quad (31)$$

where the internal leakage flow can be calculated from:

when $|y| < \left(\frac{q}{s}\right)^2 Q_l$:

$$q \cdot Q_l^2 = \frac{p_s - p_0}{2} \quad (32\text{-a})$$

when $\left(\frac{q}{s}\right)^2 \cdot Q_l \le |y| < y_{tl}$:

$$s \cdot |y|^{1/2} \cdot Q_l^{3/2} = \frac{p_s - p_0}{2} \quad (32\text{-b})$$

and when $|y| \ge y_{tl}$:

$$s y_{tl}^{1/2} Q_l^{3/2} + w(|y| - y_{tl}) Q_l = \frac{p_s - p_0}{2} \quad (32\text{-c})$$

where

$$q = \frac{0.5\rho}{K_t^2 f^2 (\sqrt{(\delta + r_s + r_b)^2 + (r_s + r_b)^2} - r_s - r_b)^2} , \quad (33)$$

$$s = \frac{23(\rho\eta)^{1/2}}{f^{3/2}\delta^{5/2}} , \quad (34)$$

$$w = \frac{12\eta}{f\delta^3} , \quad (35)$$

$$y_{tl} = \frac{0.075\delta Q_l}{\pi d_s \nu} . \quad (36)$$

2 EXPERIMENTAL VERIFICATION

The presented model was numerically solved and verified with experimental results for no-load servovalve B.31.210.12.1000.U2V - manufactured by PPT- Trstenik, Serbia (Fig. 4 and Fig. 5).

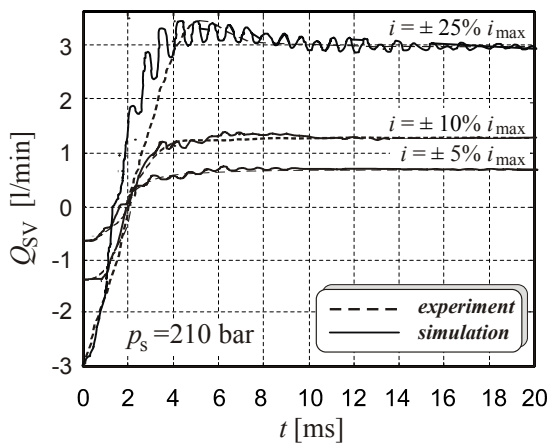

Fig. 4. *The transient response of the servovalve (square periodic input current signal – 10 Hz frequency)*

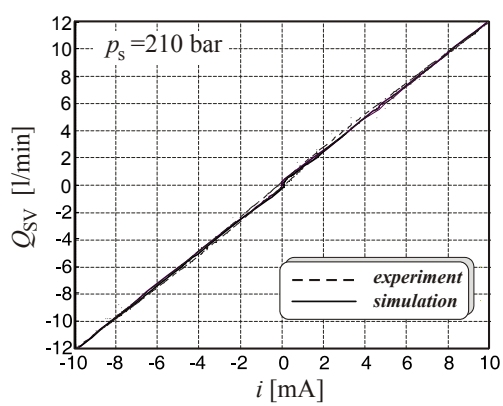

Fig. 5. *The static flow characteristic of the servovalve*

Parameter values of the servovalve are presented in nomenclature (in brackets). The manufacturer of permanent magnet provided values of parameters related to permanent magnet except its geometrical parameters, whereas values of constants related to permanent magnet and the

torque motor were calculated according to the procedure described in [5]. The friction coefficients were estimated to match the appropriate experimental transient responses. Values for other parameters were determined with a direct measurement on the disassembled servovalve. The equilibrium distance from the flapper tip to nozzles is an exception from this rule. It was calculated according to the assemblage requirement, which demands that pressures in both nozzles should be 70 bar when the supply pressure is 140 bar and when the flapper is in the zero position.

Static and dynamic experimental analyses of the servovalve were performed on the standard servovalve testing equipment, property of PPT (static – MOOG - Plotterstand D046-030, dynamic – MOOG - Frequenzgang - Pruefstand D046032).

The model satisfactory agrees with the experiment and it can be used for the sensitivity analysis.

3 SENSITIVITY ANALYSIS

Torque motor parameters relate to its electromagnetic nature are length of each air gap at null x_{p0}, permanent magnet cross sectional area A_m, torque motor gap area A_p, magnetic flux density of permanent magnet $B_{r\,m}$, permanent magnet length l_m, number of turns of each coil N, distance from armature pivot to the centre of permanent magnet pole face r and permanent magnet permeability μ_m.

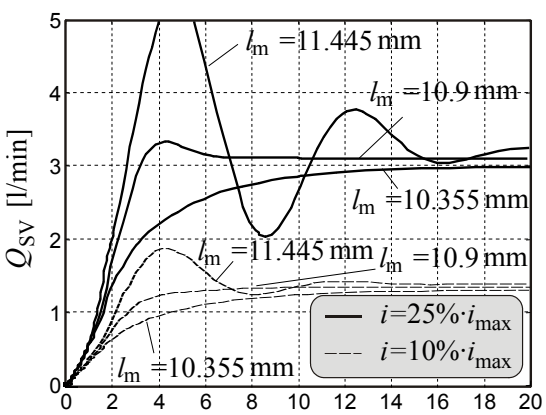

Fig. 6. *The effect of the variation of permanent magnet length on servovalve performance*

In order to analyse the influence of torque motor parameters on servovalve characteristics, the transient responses for step input current signal (from 0 to steady regimes determined with two input current signals i - 10% and 25% of the rated i_{max}) were numerically modelled. Three different values for the analysed parameters were taken in numerical modelling: value of the analysed servovalve, one higher and one smaller value. Results of the modelling are shown in Fig. 6 to 12.

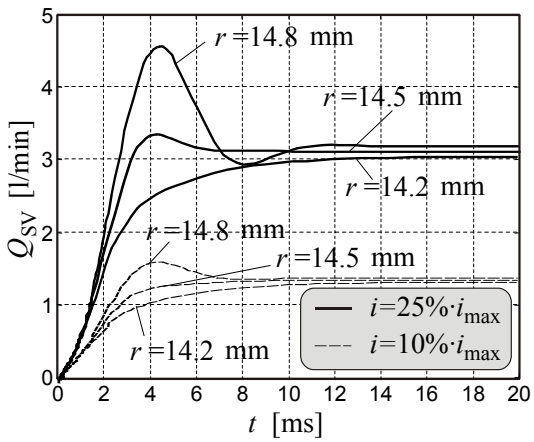

Fig. 7. *The effect of the variation of distance from armature pivot to the centre of permanent magnet pole face on servovalve performance*

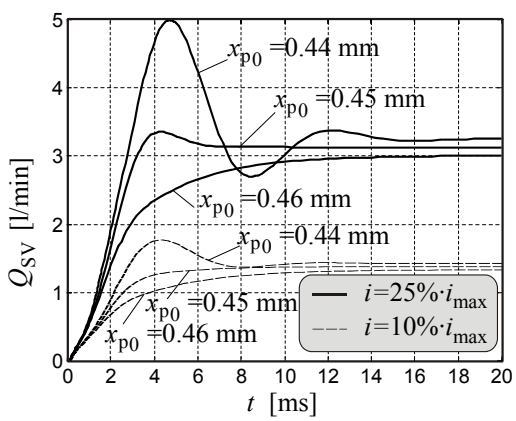

Fig. 8. *The effect of the variation of air-gap length at null on servovalve performance*

It can be noticed on diagrams that the increase (decrease) of x_{p0} generates the same effects as the decrease (increase) of other analysed parameters.

Analysing the influence of torque motor geometric parameters one can conclude that

length parameters (l_m, r, x_{p0}) have greater influence on transient response then areas (A_m, A_p). Variation of A_m has bigger influence then variation of A_p.

It is especially important to analyse the effects of variation of x_{p0}, $B_{r\ m}$ and N on servovalve performance. These three parameters can be easily modified when a designer wants to change the characteristics of an existing servovalve.

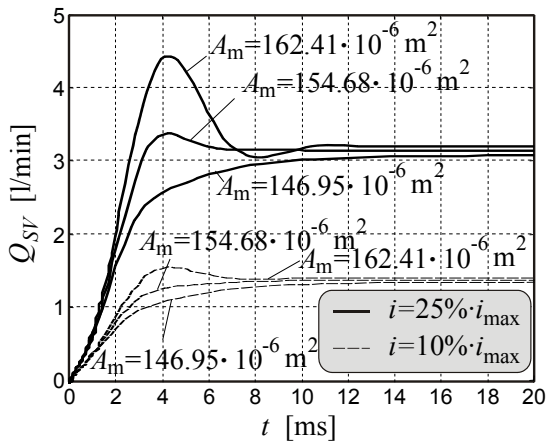

Fig. 9. *The effect of the variation of permanent magnet cross sectional area at zero on servovalve performance*

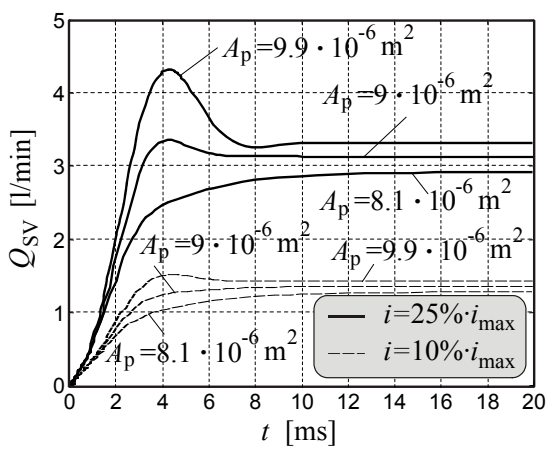

Fig. 10. *The effect of the variation of torque motor gap area on servovalve performance*

The change of air-gap length at null x_{p0} has the greatest influence on the quality of transient response and steady values of the servovalve flow (Fig 8.). Small reduction of x_{p0} value (by 2 %) induce the decrease of rise time and existence (for i=10%·i_{max}) i.e. the increase of overshoot (for i=25%·i_{max}) and finally higher the stationary value of servovalve flow. If the x_{p0} has higher value then the transient response becomes more sluggish and stationary value of servovalve flow is being reduced.

With smaller changes for the same percentage variation of parameter value, similar trend can be noticed in Fig. 11 where the value of residual magnetic flux density is changed.

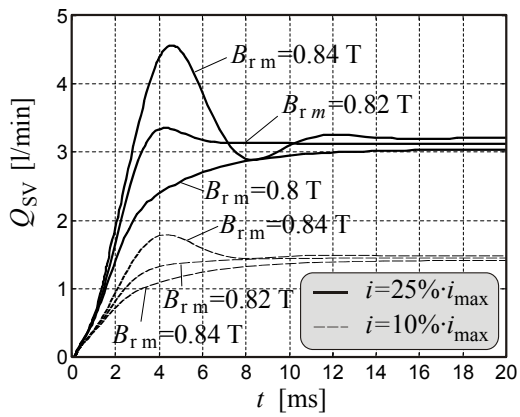

Fig. 11. *The effect of the variation of residual magnetic flux density on servovalve performance*

The change of number of turns of each coil N does not have influence on the quality of transient response. It only has small influence on the steady value of servovalve flow.

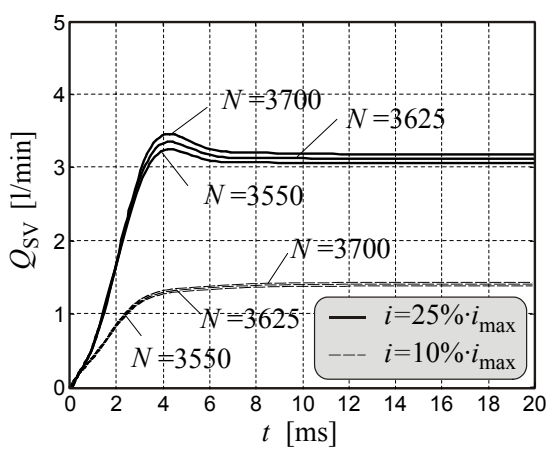

Fig. 12. *The effect of the variation of number of turns of each coil on servovalve performance*

3 CONCLUSION

Standard engineering practice considers that if servovalve designers want to redesign

existing or design a new servovalve they must modify some properties on physical object and then experimentally verify the results of this action. The model presented in the paper primarily gives a useful design tool, since all its parameters are physical quantities. When servovalve designers have such developed model that includes phenomena and parameters of influence and can predict their performance in a wide range of expected regimes, they can simply redesign existing servovalves without physical modification. They can numerically model all possible situations and choose results that are appropriate for their needs.

Using the detailed servovalve mathematical model authors analysed the influence of torque motor electromagnetic parameters. The analysis showed that the biggest influence on servovalve dynamic characteristics has variation of air-gap length at zero, although the influence of other parameters can not be neglected. Similar analysis can be performed for other servovalve parameters.

4 NOMENCLATURE

A_m	permanent magnet cross sectional area ($154.68 \cdot 10^{-6}$)	[m^2]
A_p	torque motor gap area ($9 \cdot 10^{-6}$)	[m^2]
B_{fl}	flapper bending rigidity (0.0256)	[Nm^2]
B_t	flexure tube rigidity (0.0302)	[Nm^2]
$B_{r\,m}$	magnetic flux density of permanent magnet	[T]
d_n	nozzle diameter ($0.28 \cdot 10^{-3}$)	[m]
d_o	left (right) constant orifice diameter ($0.18 \cdot 10^{-3}$)	[m]
d_{od}	drain constant orifice diameter ($0.4 \cdot 10^{-3}$)	[m]
d_s	spool diameter ($4.62 \cdot 10^{-3}$)	[m]
f	spool valve area gradient ($4.8 \cdot 10^{-3}$)	[m]
F_a	axial component of flow force on spool	[N]
F_c	dry friction force on spool	[N]
F_{c0}	initial dry friction force on spool ($3.2 \cdot 10^{-3}$)	[N]
F_{cn}	nominal dry friction force on spool ($2.2 \cdot 10^{-3}$)	[N]
F_f	force caused by mutual action of feedback spring and spool	[N]
F_h	flow force on flapper	[N]
i	total current	[A]
i_{max}	rate input current ($10 \cdot 10^{-3}$)	[A]
J_a	armature assembly moment of inertia with the respect of rotational centre ($1.68 \cdot 10^{-7}$)	[kgm^2]
K_c	contraction coefficient of spool orifice	[-]
K_f	feedback spring stiffness (1962)	[N/m]
K_i	torque motor gain	[Nm/A]
k_l	constant of leakage flux in air gap (0.27)	[-]
k_m	constant caused by the non-uniformity of magnetic field in permanent magnet (2.42)	[-]
K_m	torque motor electromagnetic spring constant	[Nm]
k_n	spool viscous friction coefficient (3800)	[kg/s]
K_{nl}	flow coefficient of the left flapper-nozzle restriction	[-]
K_{nr}	flow coefficient of the right flapper-nozzle restriction	[-]
K_{n0}	flow coefficient of the flapper-nozzle restrictions at zero	[-]
K_{od}	flow coefficient of the drain constant orifice	[-]
K_{o0}	flow coefficient of the left/right constant orifice an zero	[-]
k_r	magnetic reluctance constant (0.465)	[-]
K_t	flow coefficient of spool orifice	[-]
k_v	armature assembly viscous friction coefficient ($4 \cdot 10^{-4}$)	[Nms]
l_1	axial length between supply and actuator ports ($5.4 \cdot 10^{-3}$)	[m]
l_2	axial length between reservoir and actuator ports ($9.2 \cdot 10^{-3}$)	[m]
l_a	distance from the nozzle axis of symmetry to the axis of rotation of armature assembly ($8.75 \cdot 10^{-3}$)	[m]
l_f	feedback spring length ($13.3 \cdot 10^{-3}$)	[m]
l_{fl}	flapper length ($13 \cdot 10^{-3}$)	[m]
l_m	permanent magnet length ($10.9 \cdot 10^{-3}$)	[m]
l_t	flexure tube length ($8.5 \cdot 10^{-3}$)	[m]
M_m	permanent magnet magnetomotive force	[A]
m_s	spool mass ($3.1 \cdot 10^{-3}$)	[kg]
N	number of turns of each coil (3625)	[-]
p_0	atmospheric (reservoir) pressure (10^5)	[Pa]
p_d	drain orifice inlet pressure	[Pa]

p_l	left nozzle pressure	[Pa]
p_r	right nozzle pressure	[Pa]
p_s	supply pressure ($210 \cdot 10^5$)	[Pa]
r	distance from armature pivot to the centre of permanent magnet pole face ($14.5 \cdot 10^{-3}$)	[m]
r_b	radius of bushing control edge ($10 \cdot 10^{-6}$)	[m]
R_{mm}	permanent magnet reluctance	[H^{-1}]
$R_{m\,p0}$	reluctance of each air gap at the null	[H^{-1}]
r_s	radius of spool control edge ($10 \cdot 10^{-6}$)	[m]
T_e	torque caused by electromagnetic forces	[Nm]
T_f	torque caused by feedback spring deformation	[Nm]
T_t	torque caused by flexure tube deformation	[Nm]
V_d	drain compartment volume ($8.2 \cdot 10^{-6}$)	[m^3]
Q_l	leakage flow through spool orifices	[m^3/s]
Q_{SV}	servovalve volumetric flow	[m^3/s]
x	flapper tip displacement	[m]
x_0	distance from flapper tip to each nozzle at null ($38.5 \cdot 10^{-6}$)	[m]
x_n	distance from flapper tip to nozzle	[m]
x_{p0}	length of each air gap at null ($0.45 \cdot 10^{-3}$)	[m]
y	spool displacement	[m]
y_f	feedback spring end deflection	[m]
y_{ff}	fictive feedback spring ball displacement if there is no spool	[m]
y_i	spool orifice opening	[m]
y_{tl}	large transition length	[m]
z	half the feedback spring ball clearance ($2 \cdot 10^{-6}$)	[m]
α	jet angle in spool orifice	[°]
β	fluid compressibility ($1.9 \cdot 10^9$)	[Pa]
δ	spool in bushing radial clearance ($4 \cdot 10^{-6}$)	[m]
η	fluid dynamic viscosity (0.012)	[Pa·s]
φ	flapper free end inclination	[rad]
μ_0	magnetic permeability of vacuum	[H/m]
μ_m	permanent magnet permeability (5)	[H/m]
ν	fluid kinematic viscosity ($14 \cdot 10^{-6}$)	[m^2/s]
θ	armature deflection	[rad]
ρ	fluid density (871)	[kg/m^3]

5 REFERENCES

[1] Merritt, H. (1967) Hydraulic Control Systems, John Wiley & Sons, New York.

[2] Arafa, H. A. and Rizk, M. (1987) Identification and Modelling of Some Electrohydraulic Servo-Valve Non-Linearities. Proceedings of the Institution of Mechanical Engineers, Part C: Mechanical Engi-neering Science, vol. 201, no. 2, pp. 137-144.

[3] Wang, D., Dolid, R., Donath, M., Albright, J. (1995) Development and Verification of a Two-Stage Flow Control Servovalve Model, ASME The Fluid Power and Systems Technology Division (Publication), FPST, vol. 2, pp. 121-129.

[4] Fussell, B., Darwin, J., Prina S. (1999) Servovalve Torque Motor Analysis, Electrical Insulation Conference/Electrical Manufacturing & Coil Winding Expo, 1999.

[5] Urata, E. (2000) Study of Magnetic Circuits for Servovalve Torque Motors, Bath Workshop on Power Transmission and Control (PTMC'00), Bath, UK, pp. 269-282.

[6] Urata, E. (2007) Influence of unequal air-gap thickness in servo valve torque motors, Proceedings of the I MECH E Part C Journal of Mechanical Engineering Science, Volume 221, Number 11, 2007, pp. 1287-1297(11).

[7] Gordić, D., Šušteršič, V., Jovičić, N., Babić, M. (2004) Analysis of servovalve torque motor behaviour, Proceedings of the 29. NSS HIPNEF 2004, Vrnjačka Banja, Serbia, May, 19.-21., 2004, pp. 187-192. (in Serbian).

[8] Gordić, D., Babić, M., Jovičić, N. (2004) The modelling of a spool position feedback servovalve, International Journal of Fluid Power, vol. 5, no. 1, March 2004.

[9] Gordić, D. (2002) The Analyses of the Two-Stage Electrohydraulic Servovalves With the Spool Position Feedback, PhD thesis, University of Kragujevac, Serbia (In Serbian).